

# Thermal Transport Measurement Techniques for the Low Dimension Bulk Thermoelectric Materials

## RESUMEN

*Thermoelectric (TE) phenomena were extremely gain attention due to their directly conversion of heat energy into electrical one base on well-known Seebeck effect. Thus reason made these materials a promising way in order to harvest wasted energy and as a consequence helping the global warming. The conversion efficiency of such materials is quantified by the dimensionless figure of merit  $ZT$ ,  $TS^2/\rho\kappa$  where  $S$  is the Seebeck coefficient (or thermopower),  $\rho$  the electrical resistivity,  $\kappa$  the thermal conductivity, and  $T$  is the absolute temperature. Therefore intense studies were carried out by various groups in order to obtain high performance thermoelectric modules. It is evident that the one pair of thermoelectric will not produce considerable electric energy for daily applications. The high volumes of work were done in order to minimize the dimensions of the TE pairs so the more pairs can be placed in the single modules. However, in order to obtaining the performance of these materials we should capable of measuring the  $ZT$  parameters, among them thermal conductivity. As for today there is not any commercial system capable of measuring the thermal conductivity of so low dimensions. In this work after the exploring the different methods and techniques, a simple but practical thermal conductivity measurement system and analysis for the low dimension bulk thermoelectric materials were successfully developed.*

## Contents

I.	Introduction.....	3
1.	Thermoelectric Materials .....	4
2.	Thermoelectric Measurement Issues.....	6
2.1.	Issues: Standards and Samples .....	6
2.2.	Issues: Contacts and Contact Effects.....	7
3.	Thermal Conductivity Measurements .....	8
3.1.	Absolute Axial Heat Flow or Thermal Potentiometer .....	8
3.2.	Comparative Methods.....	10
3.3.	Steady-State Technique.....	12
3.4.	Comparative Technique.....	13
3.5.	3 $\omega$ Method.....	14
3.6.	Overview of Laser Flash Thermal .....	16
II.	Experimental Design.....	18
III.	Measurements, Results and discussions .....	20
IV.	Conclusions & Further works .....	24
V.	Reference .....	25

# I. Introduction

---

During the 1950s and 1960s, there was a considerable amount of research activity in the field of thermoelectric (TE) materials. Alloys based on the  $\text{Bi}_2\text{Te}_3$  system ( $\text{Bi}_{1-x}\text{Sb}_x$ ) $_2(\text{Te}_{1-x}\text{Se}_x)$  $_3$  and the  $\text{Si}_{1-x}\text{Ge}_x$  system were some of the most widely studied TE materials. These materials were extensively studied and optimized for their use in TE applications (solid-state refrigeration and power generation)<sup>1-3</sup>, and to date they remain the state-of-the-art materials for their specific temperature regime. Recently there has been renewed interest in the field of TEs<sup>4-6</sup>. This has been driven, in part, by new applications requiring materials that exhibit higher performance than the existing materials<sup>7-13</sup>. A distinction that is evident in this past decade of TE materials' research has been the extensive collaboration among synthesis, measurements, and theory. This synergy makes for rapid advances in the development of new materials; from theoretical prediction to solid-state synthesis, and then to the subsequent characterization of a new material. A key factor in these advances is the accurate and rapid measurement of the important properties that are related to a material's TE performance. In addition, advances in thin film and superlattice growth techniques and novel processes for forming bulk materials have allowed the exploration of a variety of new systems. There have been reports of high values of the figure-of-merit, ZT, in the thin film and superlattice materials with ZT are greater than two in some instances<sup>14, 15</sup>. Samples of this geometry and configuration exhibit specific challenges for measuring their properties.

As stated previously, one of the difficulties in investigating TE materials lies in obtaining reliable and accurate measurements of their electrical and thermal properties, such as the Seebeck coefficient or thermopower  $\alpha$ ; the electrical resistivity  $\rho$ ; and the total thermal conductivity  $\kappa$ : These terms go into the material's dimensionless figure-of-merit, ZT, which is given by

$$ZT = \frac{\alpha^2 \sigma T}{\kappa} = \frac{\alpha^2 T}{\rho \kappa}$$

Where, T is the absolute temperature in Kelvin. The total thermal conductivity,  $\kappa$  comprises two parts,  $\kappa = \kappa_L + \kappa_E$ ; which are the lattice and electronic contributions, respectively. The power factor  $\alpha^2 \sigma T$  (or  $\alpha^2 T / \rho$ ) is optimized as a function of carrier concentration (typically around  $10^{19}$  carriers/cm<sup>3</sup>), through doping, to give the largest ZT. High mobility carriers are most desirable in order to have the highest electrical conductivity for a given carrier concentration. Semiconductors have been primarily the materials of choice for TE applications. These properties, along with determination of the carrier concentration and carrier mobility from Hall effect measurements, are essential in evaluating a material for potential TE applications.

Tremendous efforts were expended in the late 1950s and 1960s in relation to the

measurement and characterization of TE materials. These efforts were made by a generation of scientists, who for the most part are no longer active, and this expertise would be lost to us unless we are aware of the great strides they made during their time. There are several recent papers that give excellent reviews of the issues related to accurate measurements of the electrical and thermal transport properties of TE materials<sup>16–19</sup>.

## 1. Thermoelectric Materials

TE energy conversion utilizes the Peltier heat generated when an electric current is passed through a TE material to provide a temperature gradient with heat being absorbed on the cold-side and rejected at the heat sink, thus providing a refrigeration capability. Conversely, an imposed  $\Delta T$  will result in a voltage or current, i.e., small scale power generation<sup>20, 21</sup>. This power generation aspect is widely utilized in deep space applications, as has been evident by NASA's recent Cassini mission and the longer-term Voyager missions. A radioactive material acts as the heat source in these fix radioactive thermoelectric generators (RTGs) and thus provides a long-lived energy supply. The advantages of TE solid-state energy conversion are compactness, quietness (no moving parts), and localized heating or cooling. Applications include cooling of CCDs, laser diodes, infrared detectors, low noise amplifiers, computer chips, and biological specimens. The essence of defining a good TE material lies primarily in determining the material's dimensionless figure-of-merit,  $ZT$ . The Seebeck coefficient or thermopower is related to the Peltier effect by  $\Pi = \alpha T = Q_P / I$  where  $\Pi$  is the Peltier coefficient,  $Q_P$  is the rate of heating or cooling, and  $I$  is the electrical current<sup>22</sup>. The efficiency ( $\eta$ ) of a TE power generation device or the coefficient of performance (COP) of a TE refrigeration device are directly related to the figure of merit of the TE material or materials. In fact,  $\eta$  and COP are proportional to  $(1+ZT)^{1/2}$ . A concise, yet thorough, overview of principles and phenomena related to TE materials is given in a recent encyclopedia of materials article<sup>23</sup>. In addition, there are a number of excellent references that discuss aspects of TE materials in more depth<sup>1–3, 24–27</sup>.

The measurements that are typically necessary to characterize a TE material are listed below in Table 1. These terms are defined as follows:

$\mu$  is the carrier mobility.

$n$  is the carrier concentration.

$L_0$  is the sample distance between the measuring leads.

$A$  is the cross-sectional area,  $R_H$  is the Hall coefficient.

$e$  is the charge of the carrier,  $-e$  (electrons) or  $+e$  (holes).

Of course, there are many other factors that go into the full understanding of the thermal and electrical transport in a material but the aforementioned properties will be given as a fundamental starting point.

The values of  $\alpha$ ,  $\rho$ , and  $\kappa_T$  that yield a  $ZT \approx 1$  for the  $\text{Bi}_2\text{Te}_3$  alloy system at  $T = 300 \text{ K}$  are roughly taken as  $\alpha = 225 \text{ } \mu\text{V/K}$ ,  $\rho = 1 \text{ m}\Omega\text{-cm}$ ,  $\kappa = 2 \text{ Wm}^{-1} \text{ K}^{-1}$ . Often, a major uncertainty lies in just the accurate determination of the electrical resistivity and thermal conductivity from resistance and thermal conductance measurements, respectively, because of uncertainty in determination of the sample dimensions. An uncertainty of 5% in sample dimensions can easily lead to 10 to 15% uncertainty in  $ZT$ <sup>18</sup>.

## 2. Thermoelectric Measurement Issues

### 2.1. Issues: Standards and Samples

One of the first steps in improving the accuracy of a particular experimental setup is to identify and quantify any systematic errors that may be evident in the measurement apparatus or technique.

TABLE 1 Correction Factor for Planar Dimensions,  $C_1(a/d)$

d/s	Circle Diam d/s	a/d =1	a/d =2	a/d =3	a/d ≥ 4
1.0	—	—	—	0.9988	0.9994
1.3	—	—	—	1.2467	1.2248
1.5	—	—	1.4788	1.4893	1.4893
1.8	—	—	1.7196	1.7238	1.7238
2.0	—	—	1.9454	1.9475	1.9475
2.5	—	—	2.3532	2.3541	2.3541
3.0	2.2662	2.4575	2.7000	2.7005	2.7005
4.0	2.9289	3.1137	3.2246	3.2248	3.2248
5.0	3.3625	3.5098	3.5749	3.5750	3.5750
7.5	3.9273	4.0095	4.0361	4.0362	4.0362
10.0	4.1716	4.2209	4.2357	4.2357	4.2357
15.0	4.3646	4.3882	4.3947	4.3947	4.3947
20.0	4.4364	4.4516	4.4553	4.4553	4.4553
40.0	4.5076	4.5120	4.5129	4.5129	4.5129
∞	4.5324	4.5324	4.5324	4.5325	4.5324

One way to do this is to develop Standards (materials with known and established TE properties) to check the apparatus and measurement techniques for accuracy and reproducibility. One can obtain standards for thermal conductivity or electrical resistivity from National Institute of Standards and Technology (NIST, formerly the National Bureau of Standards). However, the lowest thermal conductivity standard that NIST currently has available is stainless steel, that has values around  $\kappa_T = 15 \text{ Wm}^{-1} \text{ K}^{-1}$  at room temperature, an order of magnitude higher than that of a good TE material. A good standard for Seebeck measurements, is even more difficult to obtain. Thus, there are very few good TE standards existing today.

A common mistake that is often made results from calculating ZT using values of the various TE properties ( $\alpha$ ,  $\rho$ ,  $\kappa$ ,  $n$ , and  $R_H$ ) which have been measured on different samples, even if from the same ingot or batch. TE materials have often proven to be somewhat inhomogeneous, even amongst samples taken from the same batch. Therefore, it is best to perform all the measurements on the same sample. In addition, these measurements should be taken as closely together in time as possible in order to eliminate sample deterioration effects. Of course, in calculating ZT, it is also important to assure that all of the measurements are taken at the same temperature. This will minimize corrections due to strong temperature dependence of the properties of the materials that are under investigation. In general, electrical and thermal transport properties can have a very strong dependence on crystallographic direction,

sometimes by orders of magnitude. Thus, when working with single crystals or oriented polycrystalline materials, it is important to verify the crystallographic direction of the measurements that are being reported. Even “pressed pellet” polycrystalline samples can exhibit slight anisotropy in their properties and sample orientation must be consistent when measuring and comparing the different TE properties. When possible, it is better to measure more than one sample of a given material. This will help to average any possible sample differences, and possibly minimize discrepancies among various research groups and be able to more fully evaluate a given set of materials.

## 2.2. Issues: Contacts and Contact Effects

Establishing excellent electrical contacts to these TE materials is also an essential factor. Large contact resistances which result in Joule heating at the contacts [ $I^2 (R_{C1}+R_{C2})$ ] can make these TE measurements extremely difficult. In some cases, Joule heating due to contact resistance can completely cancel the desirable Peltier heat flow. In addition, if the contact resistances of the current leads differ significantly, an unwanted temperature gradient can develop due to the differences in Joule heating at the sample ends,  $\Delta T \approx \rho \approx I^2 (R_{C1}+R_{C2})$ . For the  $\text{Bi}_2\text{Te}_3$  class of materials, achieving good electrical contacts has always been an important issue. The fact that Cu or Au can readily diffuse into  $\text{Bi}_2\text{Te}_3$  requires that these materials be plated with a diffusion barrier (typically Ni) prior to attaching contact leads. Once the sample has been plated with Ni, for example, a variety of contact techniques can be used to attach leads, viz., solder (many different types and temperatures), arc welding-capacitor discharge (localized point contact; this requires a robust sample to avoid damage), metal-sputtering or evaporation (Au, Ag, or Cu, etc.), ion-implantation or diffused contacts, Ag paints (e.g., Dupont 4929e Ag paint or SPIe Ag coating for SEM), metal-plating or metal epoxies, and also needle pressure probes (e.g., Pogo™ contacts)<sup>28</sup>. Unfortunately, some of the materials of interest in TEs are susceptible to the formation of oxide layers or sample decomposition at the surface. Therefore, careful surface preparation is often one of the crucial steps in achieving good adhesion and low resistance contacts. Also, most of the potential TE materials are semiconductors, thus requiring metal–semiconductor electrical contacts. This incorporates all the problems and issues that exist in making electrical contacts between metals and semiconductors<sup>29, 30</sup>. In practice, each material will present a set of contact issues that will need to be resolved. Since poor contacts present the most likely source of error in measurement.

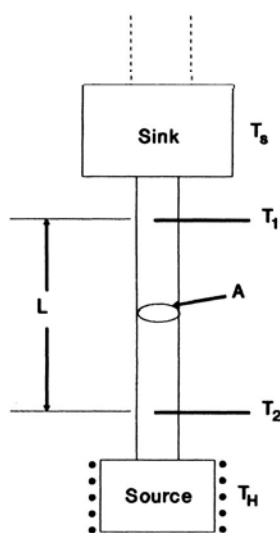
### 3. Thermal Conductivity Measurements

Thermal conductivity measurements are by far the most difficult to make with relatively high accuracy, say of the order 5%. There are many excellent papers and techniques available, which discuss in detail many of the corrections and potential errors that one, must consider<sup>2, 3, 19, 31-33</sup>.

The thermal conductivity  $\kappa_T$  of good TE materials is very low, typically  $\kappa_T \leq 2 \text{ W m}^{-1} \text{ K}^{-1}$ . This makes the measurement even more difficult since the heats will flow through other paths of higher thermal conductivity such as down lead wires and conduction by any gases or air flow around the sample. These result in an error in determination of the power input into the sample. Thus, calculating the heat loss corrections and proper thermal shielding techniques to minimize these corrections and radiation effects are critical for these TE materials.

Below room temperature, thermal conductivity is the parameter almost invariably measured either by absolute or comparative methods. Radiation transfer is conveniently small and the measurements are less susceptible to extraneous heat losses. Above room temperature heat losses become more significant and more difficult to quantify as the temperature increases. However, at room temperature, basic thermal conductivity methods are still widely used and the principal methods are described below.

#### 3.1. Absolute Axial Heat Flow or Thermal Potentiometer



This method is most widely used for measurements at low temperatures and modern equipment differs little in principle from that used by Lees more than 80 years ago<sup>34</sup>. An excellent review of the experimental requirements is given by White.<sup>35</sup> If all the heat supplied to the source  $Q (= \partial q / \partial T)$  is conducted along the rod of uniform cross section  $A$  and distance  $L$  between thermometers (Figure 1), then at any point

$$\lambda(T) = \frac{\dot{Q}}{A} \frac{\partial L}{\partial T}$$

And the mean conductivity between points 1 and 2 separated by a distance  $L$  is given by

$$\lambda(T) = \frac{\dot{Q}}{A} \frac{L}{\Delta T}$$

FIGURE 1. Schematic of axial heat flow apparatus.

Where  $\Delta T = T_2 - T_1$  This assumes that the temperature is uniform across any element



of the cross section, and that heat losses by conduction through any residual gas, by electrical leads from  $T_1$  and  $T_2$  and by radiation are negligible.

The choice of specimen geometry is dictated by the conductivity to be measured, by thermometer sensitivity, and by the maximum and minimum values of  $Q$  that can be tolerated. In practice, the length should be sufficiently great that the distance between source end 2 and sink end 1 is greater than the diameter. For low conductivity materials equilibrium times become very long unless  $L/A$  is made small. Typically for thermoelectric material, diameters of 3 to 4 mm are preferred and  $L/A \leq 10$ .

To allow as wide a temperature range as possible, the heat sink, which is loosely coupled to a refrigerator block, is coupled to an electric heater. Temperatures may be measured using either resistance<sup>36-39</sup> or thermocouples. Typical thermocouples for low-temperature use<sup>40,41</sup> are Au<sup>+</sup> 0.03% Fe/Chromel and Au<sup>+</sup> 2.1% Co vs. magnesium or copper. Various versions of this apparatus have been constructed for use on semiconductors and thermoelectric material at 300 K<sup>40, 42</sup>. As a typical example, the apparatus of Slack<sup>40</sup> is shown in Figure 2. The temperatures are determined with respect to the heat sink, the absolute temperature of which is measured by means of a helium gas thermometer bulb. The outer can is inserted into different cryogenic liquids. The post heaters serve to bring the heat sink to any temperature in the range 3 to 300 K. A vacuum of  $10^{-6}$  torr is maintained and a radiation shield minimizes radiation losses above 200 K. It is perhaps worth mentioning that a number of papers reporting low-temperature data on thermoelectric material refer to measurements made using "standard techniques" without giving more details. These are almost certainly the axial heat flow method. This technique has also been used for thermal conductivity measurements of high  $T_C$  superconductors.

Apparatus has been constructed to measure thermal conductivity above room temperature and various excellent systems have been devised<sup>43-45</sup>. The important fact here is to avoid spurious heat loss from the heaters, but more especially from the sample. The essential experimental requirement is the elimination, as far as possible, of radiation losses and this is achieved by a series of guard heaters whose temperature is matched to that of the sample. However, such equipment has been used to measure the thermal conductivity of semiconductors and thermoelectric<sup>46</sup>. However, a useful critique of measurement of thermal conductivity at high temperatures by this technique is given by Laubiz<sup>47</sup>.

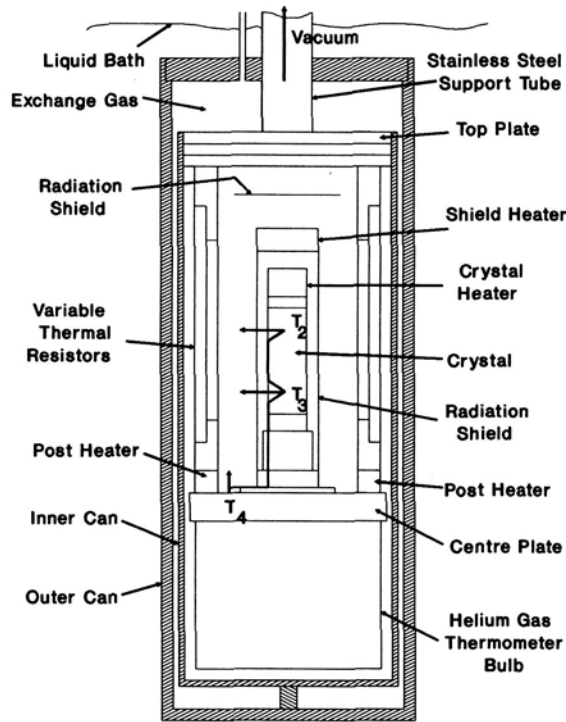


FIGURE 2. Schematic of experimental assembly for low-temperature thermal conductivity measurements

### 3.2. Comparative Methods

The comparative method determines the thermal conductivity  $\lambda$  of a material with respect to that of a suitable reference material. The unknown, whose thermal conductivity is to be measured, is sandwiched between two cylinders of a reference material of known thermal conductivity. The temperature gradients in the unknown and the standards are measured. If the cross sections are equal then

$$\lambda = \frac{\lambda_{ST}(\Delta T/\Delta X)_{ST}}{(\Delta T/\Delta X)}$$

Where  $\lambda_{ST}$  is the known thermal conductivity of the standard and  $(\Delta T/\Delta X)_{ST}$  and  $(\Delta T/\Delta X)$  are the temperature gradients of standard and test sample, respectively.

The thermocouples are usually located near the interfaces between the specimen and standards. The whole specimen-standard assembly is shielded by a matched guard heater. A typical short specimen assembly is based on the design of Francl and King<sup>48</sup>, who used Chromal/alumel thermocouples placed on silver plates separating the sample and standards. Thin layers of indium amalgam were used to overcome the problem of contact resistance. In an improved version Morris and Hust<sup>49</sup> placed the thermocouples in the sample and standards and used a heated ceramic radiation shield in three segments around sample and standards. This enabled the method to be used at temperatures up to 1000 K<sup>50</sup>. a typical assembly is shown in Figure 3.

Important design features are

1. Accurate control of heaters on the outer cylindrical guard tube to minimize radial heat losses
2. Elimination of contact resistances at interfaces by the application of pressure or heat transfer media
3. Selecting a suitable thickness of sample relative to the reference material chosen

This method does not possess the high accuracy of absolute methods and has a reported precision of -3% and an absolute accuracy of 5%<sup>51</sup>.

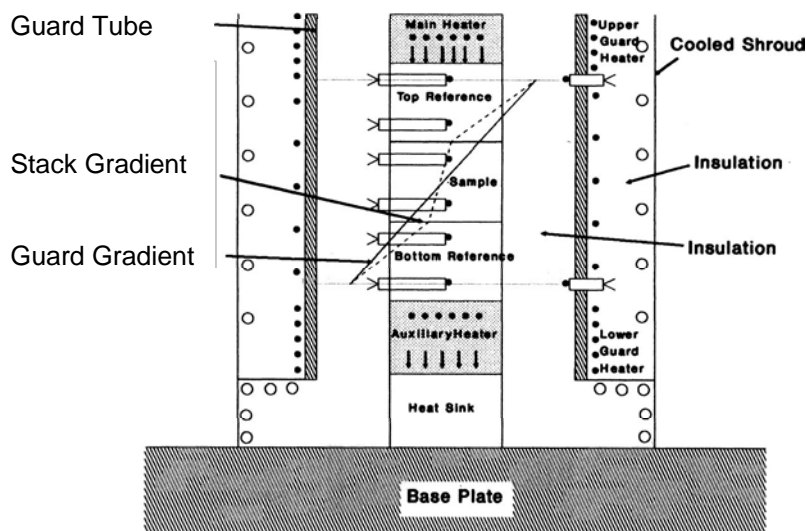


FIGURE 3. Comparative method schematic assemblies.

### 3.3. Steady-State Technique

The thermal conductivity for a typical steady-state method is given by

$$\kappa_T = \frac{Q_T L_0}{A \Delta T}$$

Where  $Q_T$  is the heating power through the sample, and  $L_0$  is the length between the thermocouple leads. A typical sample setup is shown in Figure 4. A small heater (strain gauge) is placed on top of the sample and the heating power is given by  $I^2 R$  through the heater. Phosphor bronze leads are attached to the heater. These will result in small resistive contributions and small thermal conduction losses.

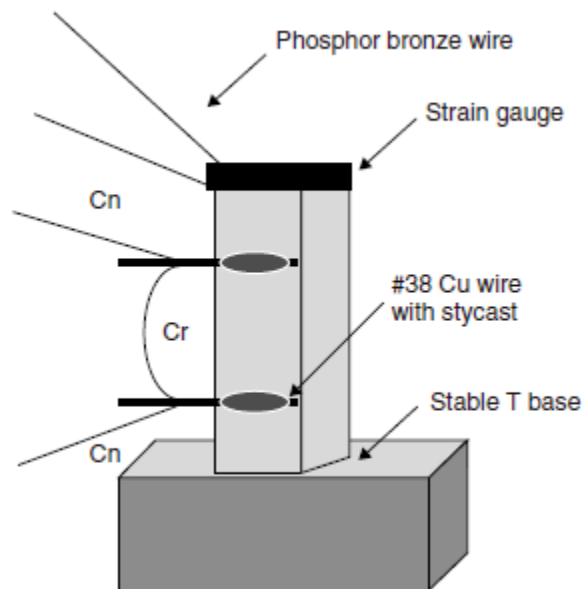


FIGURE 4 Diagram of the steady-state conductivity method used in Clemson laboratories.<sup>52</sup>

Small copper flags are attached to the sample with thermal epoxy. Small Cn –Cr thermocouple are attached to these flags to determine the temperature gradient. One can also attach small Cernox (Lake Shore Cryotronics), carbon glass, or other semiconducting thermometers to the copper flags to determine  $\Delta T$ . These are important for low temperature measurements,  $T < 10$  K, where thermocouples are rapidly losing their sensitivity. Using a temperature controller that controls the temperature stabilizes the base temperature. Power sweeps at fixed temperature yield power vs.  $\Delta T$  curves from which the slope is calculated yielding the thermal conductance of the sample. This is coupled with the sample dimension measurements to yield the thermal conductivity of the sample at a given temperature. This system is described in detail elsewhere<sup>19</sup>. Errors due to radiation loss or gain between the surroundings and the sample, convection, and conduction through any lead wires can be substantial. The radiation loss is given by

$$Q_{\text{rad}} = \epsilon \sigma_{\text{SB}} A (T_0^4 - T_s^4)$$

where  $T_0, (T_s)$  are the temperatures of the sample and the surroundings, respectively, and  $\sigma_{SB}$  is the Stephan –Boltzmann constant ( $\sigma_{SB} = 5.7 \times 10^{-8} \text{ Wm}^{-2} \cdot \text{K}^{-4}$ ) and  $\varepsilon$  ( $0 < \varepsilon < 1$ ) is the emissivity. Proper thermal shielding and thermal anchoring are essential for reliable and accurate measurements. Heat losses can also be due to convection or circulating gas flow around the sample. The best way to minimize these convection losses is to operate the measurement with the sample in a moderate vacuum ( $10^{-4}$  to  $10^{-5}$  torr). This will also reduce the heat loss due to conduction through the gaseous medium. The other substantial heat loss mechanism is due to conduction. This can be due to loss from the thermocouple or other leads attached to sample for temperature measurement. Long lead lengths of small diameter (small A) with sufficient thermal anchoring, so that essentially no  $\Delta T$  arises between the sample and shield, is important for minimizing this effect. One must accurately determine the power through the sample by considering the various loss mechanisms. Thermal resistance of leads, heaters, etc., as well as interface anchoring between the sample, the heater, and the heat sink is also important.

At times the radiation losses may be estimated by determining the temperature dependence of the lattice thermal conductivity between 50 and 150 K. If there is a distinct temperature dependence of the lattice thermal conductivity, this can be extrapolated to higher temperature, say 300 K. The difference between the calculated and measured lattice thermal conductivity can be calculated. If this difference has a  $T^3$  temperature dependence it can usually be attributed to radiation losses. This is illustrated in Figure .5 for a research sample (a half Heusler alloy) measured in the labs at Clemson. Even if one minimizes or effectively measures many of these losses, the sample length and cross-section must be accurately determined, a challenge which, can still yield 5 to 10% uncertainty. Again, measuring known standards and thoroughly calibrating the apparatus are essential. It is suggested that one uses a number of different standards with different thermal conductivity. Pyrex and Pyroceram are suggested as low thermal conductivity standards.

### 3.4. Comparative Technique

Many techniques other than the standard steady-state method are valid. In the comparative technique a known standard is put in series between the heater and the sample. This technique is best when the thermal conductivity of the standard is comparable to that of the sample. Also, the same type of errors and corrections must be considered as for the steady-state technique. The power through the standard (1) is equal to the power through the sample (2) and, given the thermal conductivity of the standard  $k_1$ , the thermal conductivity of the sample  $k_2$ , is given by

$$\kappa_2 = \kappa_1 \left( \frac{A_1 \Delta T_1 L_2}{A_2 \Delta T_2 L_1} \right)$$

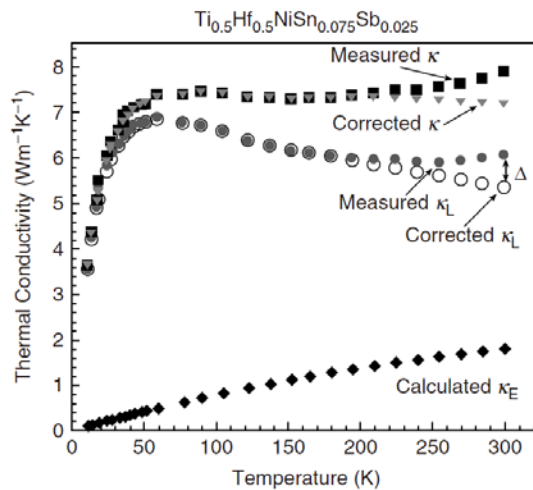


FIGURE.5 A plot of the thermal conductivity as a function of temperature is shown.  $\kappa_T$ : Total, and  $\kappa_L$ : lattice and  $\kappa_E$ : electronic.  $\Delta$ : The difference between the extrapolated and measured lattice thermal conductivity.

### 3.5. 3 $\omega$ Method

Another technique that is becoming popular for TE materials, as well as for many nonconducting low thermal conductivity systems, is the 3 $\omega$  technique<sup>53, 54</sup>. This technique was originally developed for measuring the thermal conductivity of glasses and other amorphous solids. More recently, it has been used to measure thermal conductivity in thin film samples. In this technique a thin metal strip (typically Au or Pt) is evaporated onto the sample. If the sample is an electrical conductor, then an insulating layer must be deposited prior to evaporating the metal strip. The heating produces, because of Joule heating ( $Q_J = I^2 R \approx \Delta T$ ), a temperature oscillation with frequency  $2\omega$ . The metal line also serves as a thermometer; the resistance of the line is a function of the temperature. The resistance oscillation at  $2\omega$  multiplied by the excitation current at  $V$  produces a voltage oscillation at  $3\omega$ . The amplitude of this  $3\omega$  voltage is detected by a lock-in amplifier (hence the name 3 $\omega$  method). (Figure 6.)

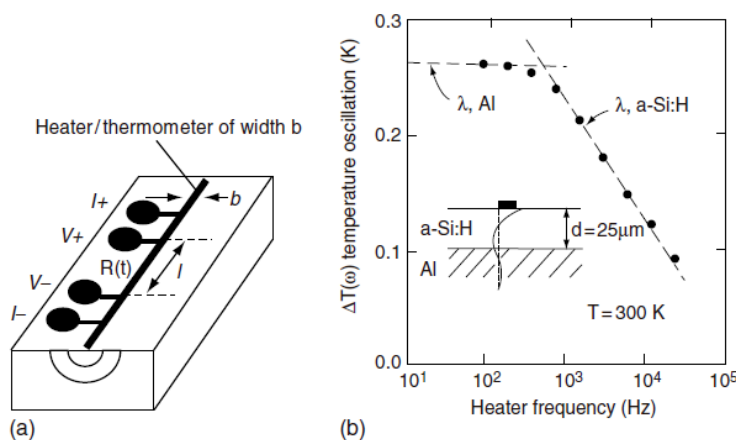


Figure 6.(a) Evaporated metal pattern on the face of a sample for 3  $\omega$  measurements; (b) amplitude of temperature oscillation of the heater/thermometer for a 25  $\mu\text{m}$  thick a-Si film on Al substrate  
In order to measure thermal conductivity, the AC voltage is monitored as a function of

the frequency of the AC applied current. The measured voltage,  $V=IR$ ; will have both an  $\omega$  component and a  $3\omega$  component. This is due to the Joule heating of the film that manifests itself in the film's resistance as a small perturbation in temperature with frequency  $2\omega$ ; i.e.,

$$V = IR = I_0 e^{i\omega t} \left( R_0 + \frac{\delta R}{\delta T} \Delta T \right) = I_0 e^{i\omega t} (R_0 + C_0 e^{i2\omega t})$$

Where  $C_0$  is a constants.

Therefore by measuring the 3rd harmonic signal at two frequencies,  $\omega_1$  and  $\omega_2$ ; the thermal conductivity is obtained by

$$\lambda = \frac{V^3 \ln(\omega_1 - \omega_2)}{4\pi I R^2 [V_3(\omega_2) - V_3(\omega_1)]} \frac{dR}{dT}$$

Where  $R$  is the average resistance of the metal line,  $V$  is the voltage across the line at frequency  $\omega$  and  $V_3(\omega_1)$ ,  $V_3(\omega_2)$ , are the voltages of the third harmonic for frequencies  $\omega_1$  and  $\omega_2$ , respectively. The slope of the metal line resistance is  $dR/dTs$ ; measured as a function of temperature.

By increasing the frequency  $\nu$ ; the technique can be adapted to measuring the thermal conductivity of films on substrates. Consider the heater/thermometer deposited on a dielectric film of thickness  $d$ ; situated on a substrate Figure 6. It can also observe that, the temperature amplitude  $\Delta T$  as a function of the frequency of the temperature oscillation  $\nu$  is shown for an amorphous silicon film (a-Si) adhered to an aluminium substrate. For small frequencies, the small slope of the straight line obtained when  $\Delta T$  is plotted vs.  $\log(\omega)$  is the result of the large thermal conductivity of the aluminium (obviously, the frequency range is inadequate to measure  $\lambda$  in this case). As the frequency increases beyond  $\sim 403$  Hz,  $\Delta T$  decreases rapidly, and approaches a straight line in Figure 6, from which the thermal conductivity of the a-Si film can be determined. The  $3\omega$  technique has many advantages. The temperature dependence of the thermal conductivity can be acquired much more readily than the steady-state technique. In addition, radiation effects are minimized with this method due to the AC nature of the measurement. Although the  $3\omega$  technique requires some level of expertise in thin film patterning and microlithography, it is generally user-friendly and inexpensive. For these reasons, the  $3\omega$  technique is probably the best pseudo-contact method available.

### 3.6. Overview of Laser Flash Thermal

Another way to measure the thermal properties of both thin-film and bulk samples is the laser flash thermal diffusivity (LFTD) method. The LFTD method measures the thermal diffusivity ( $d$ ) and the specific heat ( $CV$ ) of the sample. In this technique one face of a sample is irradiated by a short ( $\leq 1$  msec) laser pulse. Using an IR detector, the temperature rise of the opposite side of the sample is monitored. The thermal diffusivity is calculated from the temperature rise vs. time profile. The thermal diffusivity is related to the thermal conductivity as shown below:

$$d = \frac{\kappa}{DC_V}$$

Then by measuring the sample density ( $D$ ) the thermal conductivity can be determined from the following relationship

$$\kappa = dDC_V$$

To measure the specific heat of the sample simultaneous to the thermal diffusivity measurement, the absolute temperature rise of the sample must be determined for a known amount of heat input into the sample. There are many issues with this<sup>55</sup>. Anter's solution is to measure the sample relative to a known standard in the simultaneous setup. The measurement technique is illustrated in Figure 7. The time-temperature graph is shown in Figure 8, which allows the determination of the thermal diffusivity. The original method proposed by Parker assumes an isotropic and adiabatic sample (no heat loss)<sup>56</sup>. The thermal diffusivity is determined from the thickness  $L$ , of the sample and the time  $t_{1/2}$ , that the thermogram takes to reach half of the maximal temperature increase:

$$d = 0.1388 \left( \frac{L^2}{t_{1/2}} \right)$$

Since this method assumes ideal conditions of adiabatic sample and instantaneous pulse heating, it is somewhat limited in applicability. To make it more suitable to experimental conditions, other methods have been introduced over the years, which account for heat losses, finite pulse duration, nonuniform pulse heating and composite (nonhomogeneous) structures.

Commercial units are available that allow measurement of thermal diffusivity at temperatures that range from 77 K up to  $\sim 2300$  K. These units are typically automated and reasonably easy to use. Since the thermal diffusivity is related to thermal conductivity through the specific heat and sample density, i.e., the laser flash method is sometimes used to determine thermal conductivity indirectly when the specific heat and density have been measured in separate experiments. However, these systems require a relatively large sample size, a 10 to 12 mm disk for some systems. This can be difficult to obtain for a research sample.



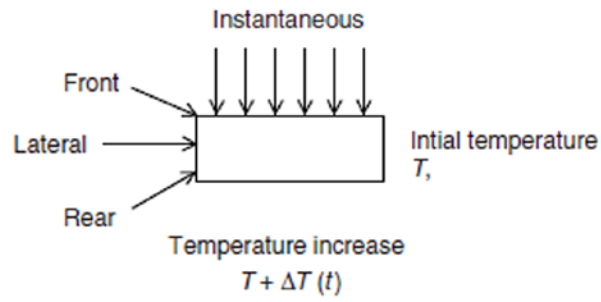


FIGURE 7 Schematic of the flash method

$$\Delta T(t) = T(t) - T_0$$

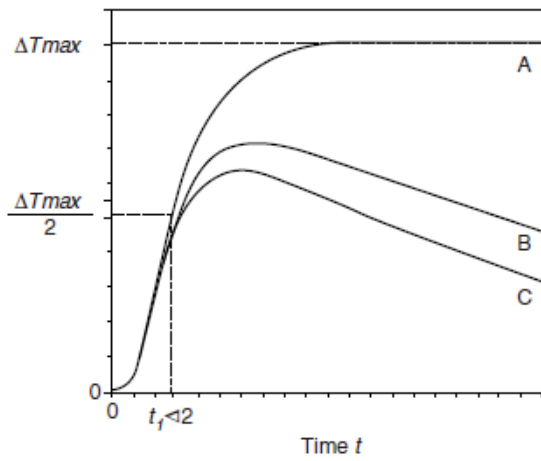


FIGURE 8. The resulting temperature increase vs. time is shown for various experimental conditions.

## II. Experimental Design

---

The experimental data was obtained using a homemade apparatus adopting Absolute Axial Heat Flow method using steady state technique. This apparatus consists of two 15Ω electric resistance heated Ni-Cr wire 0.27 mm in diameter. Both resistances were coiled in 5 mm at the two extreme ends of the sample and contacted to the sample with Epoxy thermic paste, H20E 1OZ kit. The temperature data were collected through four matched T-type thermocouples. One thermocouple was used for monitoring the room and the installation temperature  $T_{ref}$  which will be used as reference for the other three. This thermocouple was calibrated using an AHLBORN THERM-6280-2K digital thermo hygrometer, serial number D9608238 (LME-016), calibrated on 09/01/2010 by Metal test with ENAC certificate C-04582.00009. This thermocouple was attached to the copper plate using the thermal paste. The other three thermocouples were attached to the sample using the same thermic paste as wire resistance one at the centre ( $T_2$ ) and two ( $T_1$  and  $T_3$ ) in equal separation from the centre (5 mm). The aluminium sheet was used as a platform for the measurement installation and at the same time to reduce the radiation heat waste during the experiment. Furthermore, in order to avoid the convection thermal transportation through air, all the test assembly was placed in the homemade cylindrical aluminium frame with 130 mm long by 90 mm diameter by 10 mm wall thickness. This frame at one end was sealed through welding and then drilled for accommodating the data cable socket which was then welded to the wall. On the other end of the frame will be closed by an aluminium lid which has the possibility of connection to a vacuum system. The rotary vacuum system, TRIVAC D10 BHV, was used to insure the vacuum of  $10^{-4}$  torr. The features described above are shown in Figure 9 where it can be seen the position of  $T_{ref}$  thermocouple on top of the aluminium frame. Figure 10 shows the outline of sample installation which represents the version of the experimental apparatus used for the measurements.

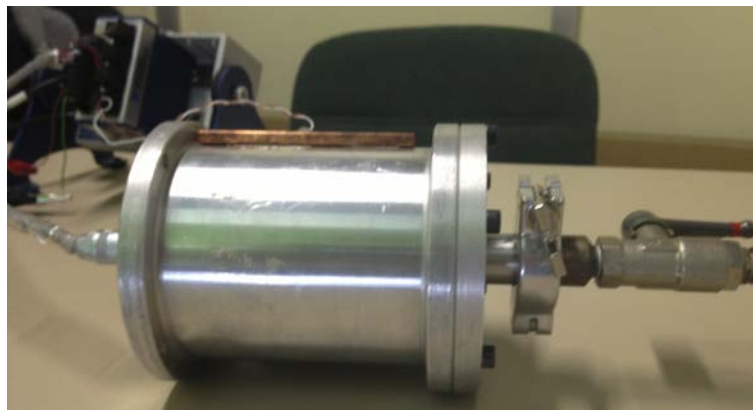


FIGURE 9. Homemade thermal measurement setup

The sample used for this test is a thermoelectric oxide  $\text{Ca}_3\text{Co}_4\text{O}_9$  which is a high homogenous cylindrical bar, produced by Laser Floating Zone technique with 2.15 mm in diameter and 40 mm length.

All the experiment was controlled by LabView 2012 national instrument homemade program which is acquiring the data through National Instrument acquisition cards. The thermocouples temperatures were measured and calibrated through NI 9219 AI Universal acquisition card. The resistances were connected to the analogue output NI 9265 national instrument AO 20 mA power supply in order to control and automate the temperature rises. However secondary external DC power supply, freak EP 613, was used, through separate channels, firstly for powering up the power supply and the starting intensity needed for heating.

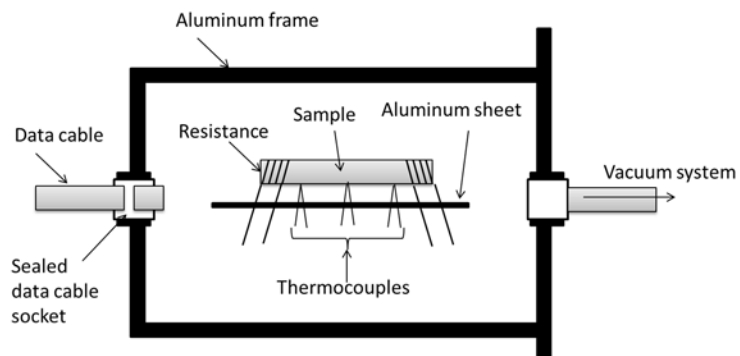


FIGURE 10 Scheme of thermal measurement system

### III. Measurements, Results and discussions

---

As the goal of this installation is observing the thermal behaviour of the low dimension samples the monitoring and measuring the temperature should be undertaken with high accuracy. For this objective series of the measurements were done and compared to insure above mentioned expectations. The calibration of  $T_{ref}$  where done in the continuous mode. Calibration curve were obtained through comparing the temperature which was registered by the  $T_{ref}$  and the thermo hygrometer. The calibration were done in the range of 0°C, ice and water, till 100 °C boiling water with interval of 1 °C per 10 min, to insure the homogeneity of temperature. So obtained calibration points were directly stored in the LabView program. In order to insure the calibration was a successful, the both apparatuses were used for monitoring the room temperature for 24 hours in the same condition that will be used for the final measurement. After the calibration  $T_{ref}$  other thermocouple were internally calibrated, through software control, and make and constantly were monitored by  $T_{ref}$ . The experiments were carried out in the steady state mode in order to make sure of the homogeneity of temperature and stability of heat flow. Furthermore in order to avoid any unwanted errors the differential analyses were applied which will be discussed in data analysis. The differential mode here is described as measuring the system one time just by one side heating and another time in the same condition but with both side heating. The resistance of electrical resistances were measured by four point test to insure the equality of the both heat sources resistance. Furthermore, in order to avoid the influence of air in the measurement the system was vacuum till  $10^{-4}$  torr for 30 min and after the vacuum, there temperature of four thermocouple were monitored for 10 min to be insure the temperature equality. Furthermore the experiment data were compared to one with the same condition but without vacuum phase.

For all the experiments and data registration, the test was performed in the same heating condition. The experiment were start at the room temperature and with 0 volts and from there in each time period the voltage were increase by 0.5 volt in the enough time period in order for make sure the steady state requirements were met.

The data obtained from first experiment were presented in Figure 11 where it was one side heating under vacuum. It can be clearly seen the rapid increasing the temperature by increasing the intensity on the side one  $T_1$ . Due to natural low thermal conductivity of the sample it can be observed the temperature increment is much lower in the centre of the sample and practically without effect on the other side. The small increment in the other side of the sample is due to the heat accumulation therefore this area is not suitable for further analysis. In order to avoid this problem, the same measurement were performed but with heating on both side, Figure 12, it can be observed the same behaviour for the middle point were temperature increase and stabled in lower values, but higher than data from previous test. The increment on temperature can be associated to second heat source and from there the thermal conductivity can be

obtained from thermal behaviour different of both measurements. For that reason, after stability of temperature the side one heating source where turn off and as was expected the  $T_2$  were decrees and stand in the same temperature as before test. From time and temperature difference in this point the thermal conductivity of the sample were calculated using steady state equations.

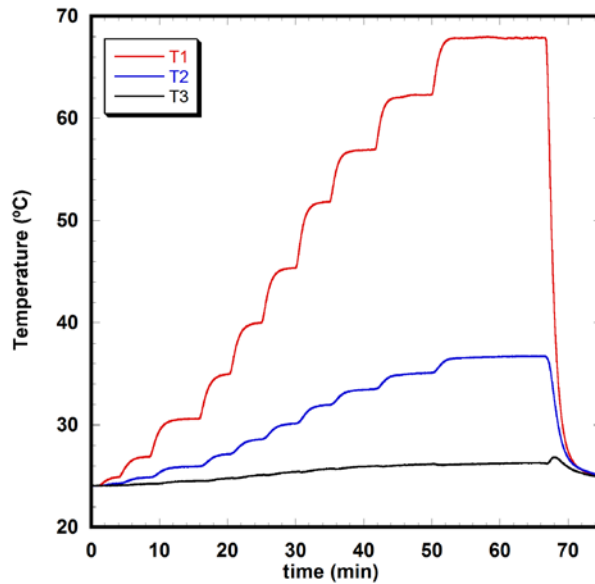


Figure11. Temperature behaviour of the sample in the one side heating test under vacuum.

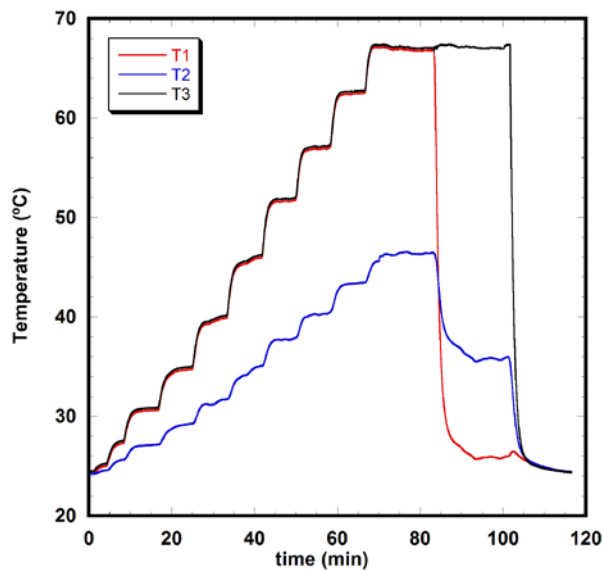


Figure12 Temperature behaviour of the sample in the two side heating test undervacuum.

$$\lambda = \frac{\Delta Q}{t} \frac{\Delta L}{A \Delta T}$$

Where A is area of the sample,  $\Delta Q/t$  is heat flow,  $\Delta L$  is distance between heat source and sample centre and  $\Delta T$  is temperature difference between the heat source and the sample centre.

$$A = (2.15 \times 10^{-3})^2 \times \pi / 4 \text{ m}^2, \quad \Delta L = 10 \times 10^{-3} \text{ m}, \quad \Delta Q/t = 5(V) \times 0.34(A) / 580 \text{ W/sec}, \quad \Delta T = 10 \text{ }^\circ\text{C}$$

Therefore  $\lambda = 0.807 \text{ W/K m}$  at  $50 \text{ }^\circ\text{C}$  (the average temperature). The so obtained value is in the same order that of the reported data for same composition for the bulk samples. This shows the reliability of the system for thermal conductivity measurement but for sample dimensions that no commercial system thus far can be measure.

In order to observe the influence of air and its presents on the measurements the two above mentioned test were carried out without vacuum stage and the results are presented in figure 13 and 14, for one side heating and two side heating measurement, respectively. The air was kept absolutely stationed during the measurement and cooling was done through aluminium frame and was observed through  $T_{ref}$ .

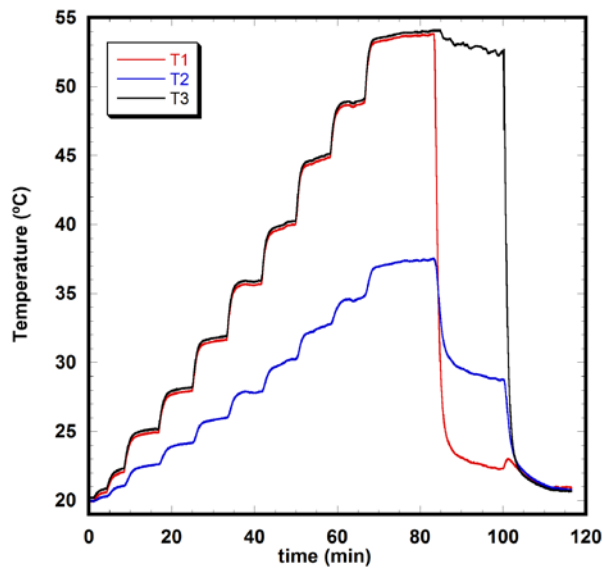


Figure13. Temperature behaviour of the sample in the one side heating test at air

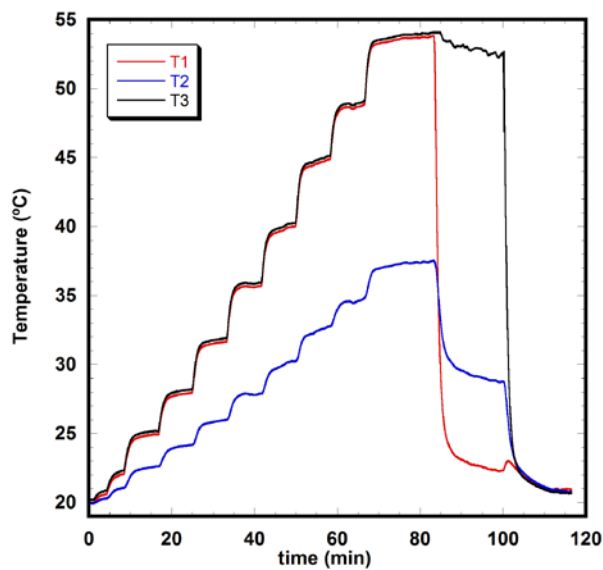


Figure14. Temperature behaviour of the sample in the two side heating test at air

It can be clearly seen that in the presence of the air all the temperatures were dropped by around 10 °C. This temperature drop is due to system cooling by air and as it can be observed by the end of the measurement the cooling rate is much faster. However due to the lower thermal conductivity of the air compared to the sample, if the same calculation were done it can be obtained the very similar values,  $\lambda = 1.02 \text{ W/K m}$  at 40 °C, a little bit higher, and at first glance it can be even surprising. But it should be taken into account 2 important facts, firstly in the first test the average temperature which is normally considered as the sample temperature is 50°C and for the second one is around 40 °C and one knowing the behaviour of the ceramic thermoelectric materials, they show higher thermal conductivity at lower temperatures. Secondly because of using the differential analysis the influence of the air will be eliminated due to its influence on the entire sample at the same time as well as heat sources.

## IV. Conclusions & further work

---

In this work the thermal conductivity measurement system have been successfully developed for measuring the thermal behaviour of low dimension specimen especially in diameter. However like all the system there are more to work one to reach the applicable system, this system is basic and can measure the sample at very limited temperature range.

Here is some recommendation that the author advise to be consider.

In order to measure the total thermal conductivity behaviour of the samples, especially the thermoelectric materials that works at high temperature, this system should be revised. The frame should be better isolated and redesign specially to lower heat transportation by radiation which it will get important at higher temperature and also the external hoven should be applied for reaching desired temperature, therefore the aluminium frame cannot be applied.

On the other hand for higher temperature the thermocouple-type should be changed and possibly the alumina tube should be applied in order to protect them.

Also the contact system should be revised so heat precipitation on the thermic paste can be avoided.

The heat source system also should be change in order to make the thermal gradient with better accuracy. And the cooling source also should be applied in order to avoid the double measurement and it corresponding errors.



## V. References

---

1. Goldsmid, H.J., *Electronic Refrigeration*, Pion Limited Publishing, London, 1986.
2. Rowe, D.M., ed., *CRC Handbook of TEs*, CRC Press, Boca Raton, FL, 1995.
3. Nolas, G.S., Sharp, J., and Goldsmid, H.J., *TEs: Basic Principles and New Materials Development*, Springer Verlag, Germany, 2001.
4. Terry, T.M., Kanatzidis, M., Mahan, G., and Lyon, H.B., Jr., eds. *Proceedings of the 1997 Materials Research Society Volume 478 TE Materials — New Directions and Approaches*.
5. Terry, T.M., Kanatzidis, M., Mahan G. and Lyon, H.B., Jr., eds. *Proceedings of 1998 Materials Research Society Volume 545 New Materials for Small Scale TE Refrigeration and Power Generation Applications*.
6. See for example other MRS proceedings on TE materials, *Proceedings of Materials Research Society Volumes 626*, (Spring 2000) *691* (Fall 2001) and *793* (Fall 2003).
7. Hicks, L.D. and Dresselhaus, M.S., Effect of quantum-well structures on the TE figure-of-merit, *Phys. Rev. B*, **47**, 12727, 1993.
8. Fleurial, J.P., Caillat, T., and Borshchevsky, A., *Proceedings of the XIII International Conference on TEs*, AIP, pp. 40 –44, 1995.
9. Sales, B.C., Mandrus, D., and Williams, R.K., Filled skutterudite antimonides: A new class of TE materials, *Science*, **272**, 1325, 1996.
10. Morelli, D.T., Caillat, T., Fleurial, J.-P., Borshchevsky, A., Vandersande, J., Chen, B., and Uher, C., Low-temperature transport properties of p type CoSb<sub>3</sub>, *Phys. Rev. B*, **51**, 9622, 1995.
11. Slack, G.A. and Toukala, V.G., Some properties of semiconducting IrSb<sub>3</sub>, *J. Appl. Phys.*, **76**, 1635, 1994.
12. Nolas, G., Slack, G., Morelli, D.T., Tritt, T.M., and Ehrlich, A.C., The effect of rare-earth filling on the lattice thermal conductivity of skutterudites, *J. Appl. Phys.*, **79**, 4002, 1996.
13. Tritt, T.M., Nolas, G.S., Slack, G.A., Ehrlich, A.C., Gillespie, D.J., and Cohn, J.L., Low-temperature transport properties of the filled and unfilled IrSb<sub>3</sub> skutterudite system, *J. Appl. Phys.*, **79**, 8412, 1996.
14. Venkatesan, R., Siivola, E., Colpitts, T., and O'Quinn, B., Thin film TE devices with high room temperature figures of merit, *Nature*, **413**, 597, 2001.
15. Harman, T., et al., Quantum dot superlattice TE materials and devices, *Science*, **297**, 2929, 2002.
16. Tritt, T.M., Measurement and characterization of TE materials. In *Materials Research Society Symposium Proceedings, TE Materials, New Directions and Approaches*, Vol. 478, T.M. Tritt, M. Kanatzidis, G. Mahan and H.B. Lyons, Jr., eds., p. 25, 1997.
17. Uher, C. and Property, T.E., Measurements, *Nav. Res. Rev., TE Mater.*, **XLVIII**, 44, 1996.
18. Tritt, T.M. Browning, V., Overview of measurement and characterization techniques for TE materials. In *Recent Trends in TE Materials Research I, Semiconductors and Semimetals*,

- Vol. 69, T.M. Tritt, ed., pp. 25– 50, 2001.
19. Tritt, T.M. and Weston, D., Measurement Techniques and Considerations for the Determination of the Thermal Conductivity of Bulk Materials. Thermal Conductivity-2004: Theory, Properties and Applications, Volume Editor T.M. Tritt, from the series Physics of Liquids and Solids, Kluwer Academic Press, New York, 2005.
  20. Tritt, T.M., TEs run hot and cold, *Science*, 272, 1276, 1996.
  21. Disalvo, F.J., TE cooling & power generation, *Science*, 285, 703, 1999.
  22. All the “Q terms” discussed in this paper will relate to rate of heat transfer or power related to that phenomenon.
  23. Tritt, T.M., TE Materials: structure, properties and applications. In *Encyclopedia of Materials Science and Technology*, Vol. 10, K.H.J. Buschow, R.W. Cahn, M.C. Flemings, B. Ilshner, E.J. Kramer and S. Mahajan, eds., pp. 1 –11. Elsevier Press LTD, Oxford, Major Reference Works, London, 2002.
  24. Wood, C.W., Materials for TE energy conversion, *Rep. Prog. Phys.*, 51, 459 –539, 1988.
  25. Mahan, G.D., Good TEs. In *Solid State Physics*, Vol. 51, H. Ehrenreich and F. Spaepen, eds., p. 81. Academic Press, London, 1998.
  26. Rowe, D.M. and Bhandari, C.M., *Modern TEs*, Reston Publishing Co., Reston, VA, 1983.
  27. Egli, P.H., ed., *TEity*, John Wiley and Sons, New York, 1960.
  28. Dupont 4929e is a product of Dupont Corporation, SPle Ag coating for SEM is a product of Dupont Corporation, Pogoe contacts are a product of Augat-Pylon Corporation.
  29. Runyan, W.R. and Shaffer, T.J., *Semiconductor Measurements and Instrumentation*, 2nd ed. McGraw-Hill, New York, 1997.
  30. Streetman, B.G., *Solid State Electronic Devices*, 4<sup>th</sup> ed. Prentice Hall, Englewood Cliffs, NJ, 1995.
  31. Parrott, J.E., and Stuckes, A.D., *Thermal Conductivity of Solids*, Pion Limited Press, London, 1975.
  32. Slack, G.A., *Solid State Physics*, Academic Press, New York, 1979.
  33. Glassbrenner, C.J. and Slack, G.A., Thermal conductivity of silicon and germanium from 30 K to the melting point, *Phys. Rev.*, V, 134, 1964.
  34. Lees, C.H., Conductivities of methods and alloys at low temperatures, *Philos. Trans. R. A*, 208,301, 1908.
  35. White, G.K., Measurement of solid conduction at low temperature, in *Thermal Conductivity*, 1, Tye, R.P., Ed., Academic Press, London,
  36. Black, W.C., Rosch, W.R., and Wheatley, J.C., Speer carbon resistors as thermometers for use below Rev. *Sci. Instrum.*, 35, 587, 1964.
  37. Gabelle, T.H., and Hull, G.W., Germanium resistance thermometers suitable for low temperature calorimetry, *Rev. Instrum.*, 28, 96, 1957.
  38. Lindenfield, P., Carbon and semiconductor thermometers for low temperatures, in *Temperature Its Measurement and Control in Science and Industry*, 3, Part 1, C.M., Ed., Reinhold, New York, 399, 1962.

39. Kelvin, M.V., Phonon scattering in sodium chloride containing oxygen, *Phys. Rev.*, 122, 1393, 1961.
40. Slack, G.A., Thermal conductivity of    and crystals, *Phys. Rev.*, 122, 1451, 1961.
41. Berman, R., Brock, J.C.F., and D.J., Properties of gold + 0.03 at% iron thermoelements between 1 and 300°K and behaviour in a magnetic field, *Cryogenics*, 4, 233, 1964.
42. Brinson, M.E. and W., Thermal conductivity and thermoelectric power of heavily doped n-type silicon, *J. Phys. C Solid State Phys.*, 3, 483, 1970.
43. Ditmars, D.A. and D.C., Thermal conductivity of beryllium oxide from 40° to J. Res. Natl. Bur. Stand., 59, 93, 1957.
44. Armstrong, L.D. and Dauphine, T.M., Thermal conductivity of metals at high temperatures. I. Description of the apparatus and measurements on iron, *Can. J. Res. A*, 25, 357, 1947.
45. Powell, R.W. and Tye, R.P., Thermal and electrical conductivities of nickel-chromium (Nimonic) alloys, *Engineer*, 209, 729, 1960.
46. Busch, G. and Steigmeier, E.F., Thermal and electrical conductivities, Hall effect and thermoelectric power of *Helv. Phys.* 34, 1, 1961.
47. Laubitz, M.J., Measurement of thermal conductivity of solids at high temperature by using steady state linear and quasi-linear heat flow, in *Thermal Conductivity*, Vol. 1, Tye, R.P., Ed., Academic Press, London, 1969, 1 11.
48. Francl, J. and W.D., Thermal conductivity. IV. Apparatus for determining thermal conductivity by a comparative method, *J. Am.* 37, 80, 1954.
49. Morris, R.G. and Hust, J.G., Thermal conductivity measurements of silicon from to *Phys. Rev.*, 124, 1426, 1961.
50. Morris, R.G. and Martin, J.C., Thermal conductivity measurements of silicon from 680 to J. *Appl. Phys.*, 34, 2388, 1963.
51. Mirkovich, V.V., Comparative method and choice of standards for thermal conductivity determination, *J. Am.* 48, 387, 1965.
52. Pope, A.L., Zawilski, B.M., and Tritt, T.M., Thermal conductivity measurements on removable sample mounts, *Cryogenics*, 41, 725, 2001.
53. Cahil, D., Thermal conductivity measurement from 30 to 750 K: the 3v method, *Rev. Sci. Instrum.*, 61, 802, 1990, and references therein.
54. Cahill, D., Katiyar, M., and Abelson, R., Thermal conductivity of a-SiH thin films, *Phys. Rev. B*, 50, 6077 –6081, 1994.
55. Anter Technical Note #71, Anter Corporation, Pittsburgh, PA (<http://www.anter.com>).
56. Parker, J.W., et al., *J. Appl. Phys.*, 32, 1679, 1961.